

Deuteron properties using a truncated one-pion exchange potential

D. W. L. Sprung, W. van Dijk,* E. Wang,[†] and D. C. Zheng[‡]

Department of Physics and Astronomy, McMaster University, Hamilton, Ontario, Canada L8S 4M1

P. Sarriguren

*Instituto de Estructura de la Materia del Consejo Superior de Investigaciones Científicas,
Serrano 119, E-28006 Madrid, Spain*

J. Martorell

Departament d'Estructura i Constituents de la Materia, Universitat de Barcelona, Barcelona, Spain

(Received 16 December 1993)

Deuteron properties are studied using the one-pion exchange potential truncated at a radius R , with a constant interior potential. The spectrum of bound states and their properties are put in evidence. We discuss the relation of this model to more realistic models of the nucleon-nucleon interaction.

PACS number(s): 21.30.+y, 21.45.+v, 21.10.Dr

I. INTRODUCTION

It is a well established fact of nuclear physics that the long-range part of the nucleon-nucleon interaction is due to one-pion exchange (OPE). Hence, all of the usual nonrelativistic potential models include the one-pion exchange potential (OPEP) as the asymptotic part of the potential. Since the deuteron is primarily a loosely bound neutron-proton system, with a rms radius 1.95 fm, one should expect that its properties are to a large extent determined by the OPEP, providing that the remainder of the potential is adjusted to give the correct binding energy. This expectation was put on a firm footing by Klarsfeld *et al.* [1] in a model-independent way. Using only the OPEP beyond $R = 1.6$ fm, they established close correlations among various deuteron properties.

Early work by Glendenning and Kramer [2] showed that using only the OPEP outside $R = 0.4915$ fm, and a hard core inside, one could fit $J = 1$ phase parameters and deuteron properties reasonably well. More recently, Friar *et al.* [3] and Ballot *et al.* [4] used a regularized OPEP, which becomes repulsive inside 1 fm, and surveyed carefully the extent to which this simple model could account for the experimental data. The present paper is an extension of this line of investigation.

In the past decade it has become accepted that nucleons are composite objects built from quarks. A number of attempts have been made to determine the short-range

part of the nucleon-nucleon interaction on this basis. In some of these, such as the P -matrix method (PMM) or the boundary condition model (BCM), the short-distance information is expressed by a boundary condition on the N - N wave function at a distance R of order 0.7–1.4 fm. Outside this radius a potential acts, which incorporates the OPEP as one of its main ingredients. The quark compound bag (QCB) is a similar but more complex model. In the above cases, the deuteron wave function is the ground state of the resulting potential, just as it is in the classic nonrelativistic potential models. Other authors [5, 6] have proposed that the deuteron should be the first excited state of the potential, the deep lying ground state representing a state forbidden by the Pauli principle acting on the quarks within the nucleons. This is in analogy to alpha-alpha scattering [7]. The alphas are bosons, but because they are made of nucleons, they cannot overlap completely without violating the Pauli principle. This phenomenon is also discussed in connection with supersymmetric quantum mechanics and nucleon-alpha scattering [8]. We shall see that our truncated OPEP model can provide a simple example of this type of wave function as well.

In this paper we discuss a simple model of a truncated OPEP, with a central flat potential in the interior. The cutoff radius and the potential depth are adjusted in all cases to give a bound state at the deuteron binding energy. While this is not a realistic model of the nucleon-nucleon interaction, it does incorporate its most important features, and it is an interesting exercise in quantum mechanics to observe the behavior of a system with strong channel coupling.

In Sec. II, we study the spectrum of the truncated OPEP in the coupled 3S_1 - 3D_1 states. The nodal structure of the various wave functions is examined in Sec. III. In Sec. IV, we draw out the analogy between this simple potential and the more realistic models mentioned above. Section V contains the conclusions.

*Permanent address: Redeemer College, Ancaster, Ontario, Canada L9K 2J4.

[†]Now at Department of Physics, University of Waterloo, Waterloo, Ontario, Canada N2L 3C5.

[‡]Now at Department of Physics, University of Arizona, Tucson, Arizona 85721.

II. TRUNCATED OPEP

A. Zero cutoff

The potential we consider is

$$V = V_C + V_T S_{12}, \quad (1)$$

with

$$\begin{aligned} V_C(r) &= V_0, \quad r < R \\ &= -f^2 \mu c^2 \frac{e^{-\mu r}}{\mu r}, \quad r > R, \end{aligned} \quad (2)$$

and

$$\begin{aligned} V_T(r) &= 0, \quad r < R \\ &= -f^2 \mu c^2 \frac{e^{-\mu r}}{\mu r} \left[1 + \frac{3}{\mu r} + \frac{3}{(\mu r)^2} \right], \quad r > R. \end{aligned} \quad (3)$$

For consistency with previous work [2], we adopt the values $f^2 \mu c^2 = 11.156184$ MeV, and $\mu^{-1} = 1.415$ fm. In the calculations we use $m/\hbar^2 = 0.024113235$ MeV⁻¹ fm⁻², where m is the nucleon mass, and for convenience we set the potential equal to zero for distances larger than 15 fm. Notice that inside the truncation radius R , the potential is purely central. We will be interested in certain intervals of R while varying the depth V_0 of the core potentials. We require that there be a bound state at energy $E = -B$. When this is the only bound state (as in the case of conventional potential models), we are dealing with the first or nodeless branch of our parameter space. When the deuteron is the first excited state, we say that we are dealing with the second branch, and so on.

To begin we shall take $V_0 = 0$. Inside R , the wave function is a spherical Bessel function for both the S -wave and D -wave components, $u(r)$ and $w(r)$, respectively. To look for a bound state solution, we solve the coupled Schrödinger equations in the region $r > R$, and match to the plane-wave boundary condition at R .

If $R > 1.055$ fm, the truncated OPEP above is too weak to support a bound state. As R decreases, a bound state appears, and reaches the deuteron energy $E = -B = -2.224575$ MeV, at $R = 0.87492058$ fm. (The large number of digits quoted is required to accurately reproduce the desired energy, due to the great depth of the OPEP.) This state continues to descend as R decreases further. A second bound state appears when R is about 0.3 fm, and it reaches $-B$ at $R = 0.28122338$ fm, at which point the ground state has reached -1400.638 MeV. At $R \simeq 0.15$ fm, a third bound state appears. At these distances, the OPEP is very strong, due to the r^{-3} singularity of the tensor force, and so the wavelength is tending rapidly to zero. As $R \rightarrow 0$, an infinite number of bound states will appear. The origin would be an essential singular point of the wave equation, if the OPEP were continued into $R = 0$. But for any small but finite cutoff, the problem will have a large but finite number of solutions. Some of these are illustrated in Fig. 1. Deuteron wave functions for potentials with different cores corresponding to the first five branches are drawn in Fig. 2. We see that unlike for the nodeless state, all the others are essentially the same in the region where the OPEP

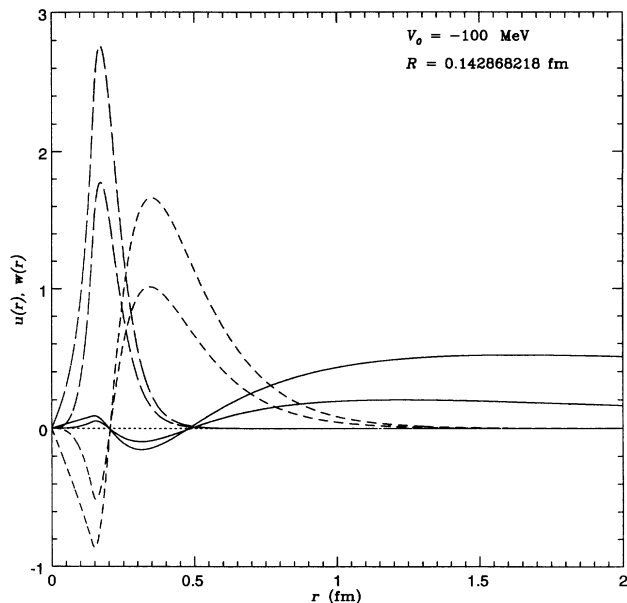


FIG. 1. Wave functions of a potential that supports three bound states, the ground state at -17155.85 MeV (long dashes), the first excited state at -1445.837 MeV (short dashes), and the second excited state at the deuteron energy (solid line). The function $u(r)$ has the larger amplitude in each case.



FIG. 2. Wave functions of the zero cutoff potentials. The solid curves correspond to $R = 0.87492058$ fm, the long-dashed curves to $R = 0.28122338$ fm, the short-dashed curves to $R = 0.14280106$ fm, and the dotted curves to $R = 0.086796284$ and 0.05842348 fm.

applies to them. In particular, they all show nearly coincident nodes in both the S - and D -wave components, at 0.48 fm. The other deuteron properties, listed in Table I, are likewise independent of the number of nodes, once one fixes the binding energy.

The stability of the wave function inside 0.5 fm can be ascribed to the dominant role of the tensor coupling of $u(r)$ and $w(r)$ at these short distances. This is analyzed in some detail in the Appendix. Even at large distances, it was argued by Ericson and Rosa-Clot [9] that $w(r)$ is largely determined by the coupling term $\sqrt{8}V_T(r)u(r)$ acting as a driving force. But at short distances, the singular nature of $V_T(r)$ makes $w(r)$ play the same role in determining $u(r)$, with the result that both components are in phase and nearly equal inside the outermost node.

B. Internal repulsion

We now let V_0 be positive, giving a (finite) repulsive core. For the nodeless branch, R decreases from 0.874 920 58 fm to 0.481 511 865 fm, as V_0 rises from zero to infinity (hard core), to maintain $E = -B$. The latter solution is potential 1 of Glendenning and Kramer [2]. For the higher branches, R is much more rigid. For the second branch, R need only decrease by 0.08 fm to 0.200 988 28 fm, with an infinite hard core. This is because of the great strength of the OPEP in the narrow deep pocket outside R . The corresponding wave functions, plotted in Fig. 3, again show striking similarity for $r > R$, and differ negligibly from those of the case $V = 0$. If one lays the drawings on top of each other, one cannot see a difference. This shows that for a given binding energy, the outer wave function is determined primarily by the truncated OPEP, and is almost independent of the inner potential.

C. Internal attraction

For the branches other than the first, a very minor increase of R is sufficient to compensate for a decrease of V_0 to -1000 MeV. The wave functions again show a similar stability as in the case of internal repulsion.

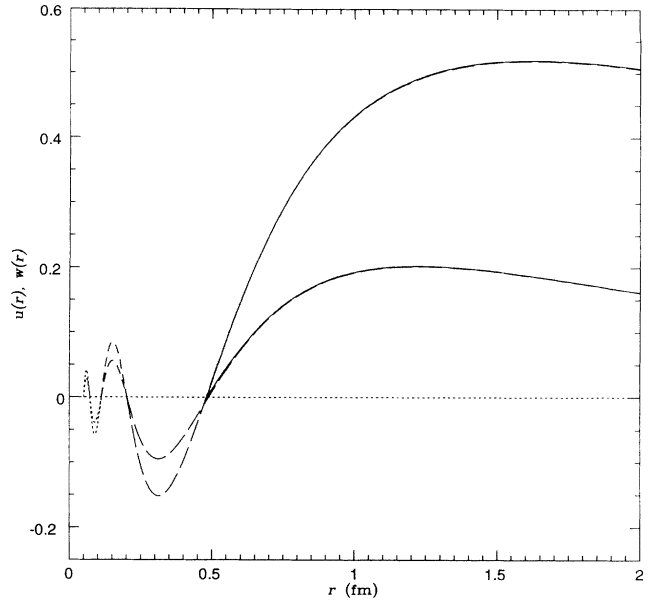


FIG. 3. Wave functions of OPEP's with a hard core. The core radii are $R = 0.481511865$ fm (solid curve), 0.20098828 fm (long-dashed curve), 0.111742741 fm (short-dashed curve), 0.07142390365 fm (dotted curve), and 0.04967366375 fm (dotted curve).

The first branch reveals more interesting behavior which we now discuss. A square well of radius 1 fm by itself can provide significant attraction. As V decreases in steps of 10 MeV, R increases, by 0.016 fm as V_0 decreases from 0.0 to -10.0 MeV and by about 0.05 fm as V_0 goes from -40.0 to -50.0 MeV. For $V_0 = -30$ MeV, we find two solutions for R , an $R_- = 0.9334281$ fm and $R_+ = 2.18939255$ fm. For the larger R , the square well provides most of the binding, as shown by the reduced values of the properties P_D , Q , and η in Table II. As V_0 further decreases, R_- approaches R_+ , and the two meet for V_0 just under -58.966 MeV. A deeper V_0 gives a bound state deeper than the required $-B$ and no solution is possible. Table II shows clearly the transition

TABLE I. Deuteron properties of the OPEP plus core potential. The binding energy is 2.224 575 MeV in each case; the quantity n is the number of nodes in the wave function.

V_0	R (fm)	n	η	P_d (%)	r_D (fm)	Q_D (fm ²)	A_s (fm ^{-1/2})	ρ_α (fm)
0	0.87492058	0	0.026583	5.9779	1.9378	0.27623	0.87004	1.67743
0	0.28122338	1	0.027116	7.4599	1.9477	0.28633	0.87405	1.70167
0	0.142801106	2	0.027114	7.4949	1.9483	0.28649	0.87433	1.70335
0	0.086796284	3	0.027114	7.4997	1.9484	0.28652	0.87437	1.70359
0	0.05842348	4	0.027114	7.5008	1.9484	0.28652	0.87438	1.70365
∞	0.481511865	0	0.027119	7.4132	1.9533	0.28800	0.87657	1.71671
∞	0.20098828	1	0.027114	7.4873	1.9490	0.28670	0.87465	1.70527
∞	0.111742741	2	0.027114	7.4978	1.9486	0.28657	0.87445	1.70406
∞	0.07142390365	3	0.027114	7.5002	1.9485	0.28654	0.87441	1.70380
∞	0.04967366375	4	0.027114	7.5009	1.9484	0.28653	0.87440	1.70373
∞^a	0.44263936	0	0.025352	7.0494	1.9216	0.26650	0.86387	1.63938
Experimental values			0.0268(7)		1.950(3)	0.2859(3)	0.8846(8)	1.764(5)

^a In this case the OPEP is multiplied by 0.9. See discussion in Sec. IV.

TABLE II. Deuteron properties of the OPEP plus core potential of different depths. The deuteron wave functions have no nodes.

R (fm)	V_0 (MeV)	η	P_d (%)	r_D (fm)	Q_D (fm ²)	A_s (fm ^{-1/2})	ρ_α (fm)
0.8906313	-10.00	0.02653	5.862	1.9366	0.2751	0.86952	1.674
0.9095809	-20.00	0.02645	5.721	1.9351	0.2737	0.86891	1.670
0.9334281	-30.00	0.02636	5.542	1.9333	0.2719	0.86815	1.666
0.9656522	-40.00	0.02622	5.299	1.9309	0.2693	0.86718	1.660
1.0162786	-50.00	0.02597	4.921	1.9275	0.2650	0.86583	1.652
1.1751603	-58.966	0.02505	3.821	1.9209	0.2508	0.86347	1.637
1.1801612	-58.966	0.02502	3.789	1.9208	0.2503	0.86345	1.637
1.4973470	-50.00	0.02265	2.180	1.9287	0.2207	0.86870	1.669
1.7886961	-40.00	0.02020	1.290	1.9561	0.1943	0.88321	1.755
2.1893925	-30.00	0.01682	0.627	2.0141	0.1609	0.91354	1.922
2.8831722	-20.00	0.01172	0.183	2.1446	0.1125	0.98415	2.253
4.7528665	-10.00	0.00384	0.007	2.5660	0.0377	1.24926	3.036

from a primarily OPEP-dominated solution at $R = 1$ fm to primarily square-well-dominated solutions at $R > 1.3$ fm. This behavior of the first branch serves to emphasize that the other branches are indeed cases where the bound state properties are dominated by the OPEP and essentially independent of the interior potential, in the sense that a minor adjustment of the cutoff radius R will compensate for any interior potential.

III. NODAL STRUCTURE OF THE DEUTERON WAVE FUNCTION

The potential models studied in the previous section all yield wave functions that have the same number of nodes in u and w . Further, as seen in Figs. 1–3, the positions of the nodes appear to be quite fixed. For a given interior potential, as one moves from branch two to the higher branches, new nodes appear at smaller radii, but the remaining nodes coincide (very nearly) with the nodes of the lower branch wave functions. A realistic potential model, which also has an additional deep bound state, is the Moscow potential [5, 6]. Its deuteron wave function has one node in u , but none in w . In this section we further clarify the possible nodal structure of the deuteron wave function for potentials of the type given by Eq. (1).

We consider the V_0 versus R relationships for the different branches. Figure 4 shows the V_0 - R relationship for the deuteron being the ground state. The curve has a minimum at around 1.2 fm, which was discussed in the previous section as the transition from domination by the OPEP to square-well domination. All wave functions of this branch are nodeless.

In Fig. 5 a similar curve is plotted for the deuteron as the first excited state. It has roughly the same shape, but is much deeper and displaced toward smaller values of R . For $R < 0.4$ fm both u and w have a single node, whereas for $R > 0.4$ fm u has a node, but w does not. The latter case yields wave functions with the same nodal structure as that given by the Moscow potential. Whereas in the previous case the D -state probability decreased as larger values of R were chosen, now the D -state probability increases to nearly 100% when R exceeds 4 fm. Nevertheless, when V_0 is less than -1500 MeV reasonable D -state

probabilities are obtained for values of R up to 0.6 fm.

The nodal structure becomes more complex for the third branch, shown in Fig. 6, and the fourth branch, Fig. 7. The three-bound-state case has reasonable D -state probabilities up to $R = 0.3$ fm. Beyond that P_D increases to a maximum of 18% at $R = 0.75$ fm and then for larger values of R drops to zero. The deuteron properties of a sample of potentials with three bound states are listed in Table III. The fourth branch has two intervals of R for which reasonable deuteron properties are obtained, i.e., $R < 0.18$ fm and $0.4 < R < 0.6$ fm. In the first interval, u and w have three or fewer nodes, whereas in the second interval u has two nodes, but w has zero or one nodes. For these intervals the wave function can have quite different behavior for radial distances less than 0.5 fm, but they are virtually identical for larger distances (see Fig. 8). For large values of R the fourth-branch wave function is predominantly D state.

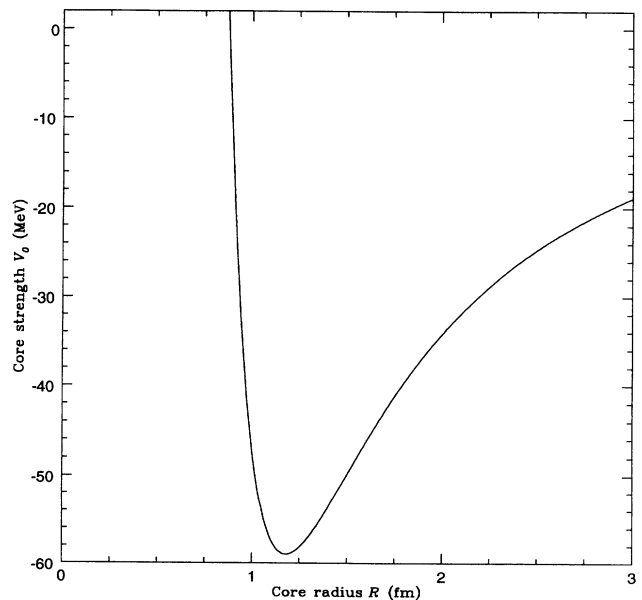


FIG. 4. The V_0 versus R relationship for potentials having the deuteron as the ground state. The wave functions have no nodes.

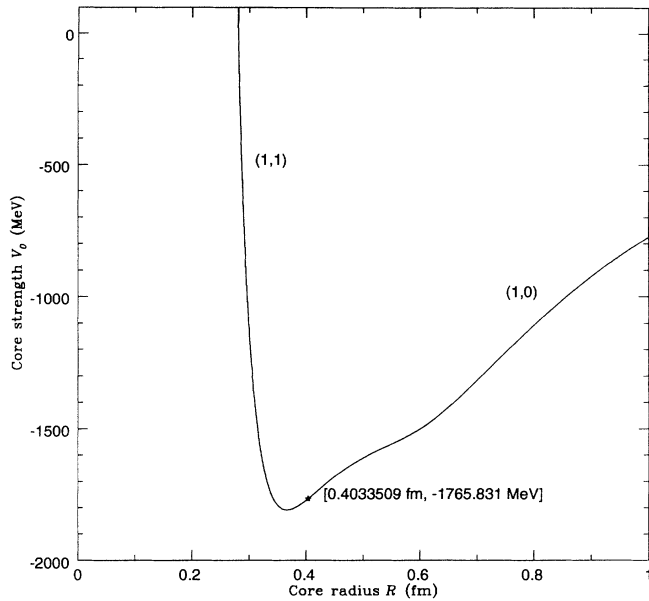


FIG. 5. The V_0 versus R relationship for potentials having the deuteron as the first excited state. The nodal character of the wave functions are indicated in parentheses (i.e., number of u nodes, number of w nodes), and the transition points, giving the core radius and strength at which the number of nodes changes, are given in the square brackets.

In each branch, potentials with cores of the shortest range generate deuteron wave functions with an equal number of nodes in the u and w functions. For such short distances the tensor force is the dominant component of the interaction and the mechanism mentioned in Sec. II A explains the similarity of the two functions. At larger distances however the strong central core is capable of producing situations in which the two functions

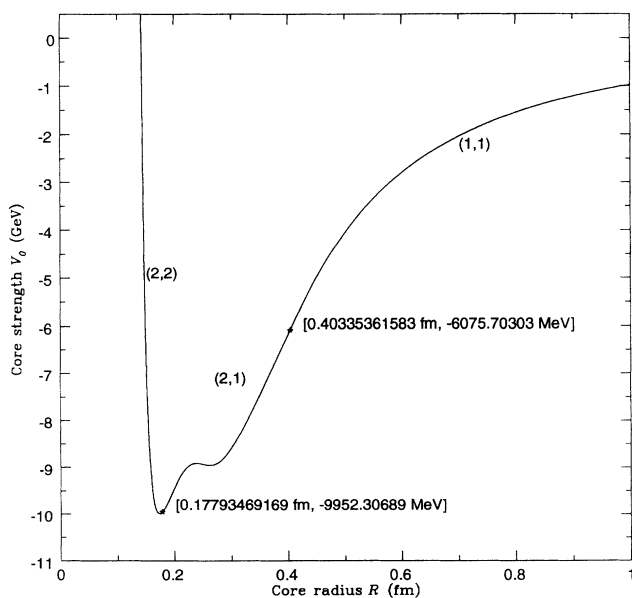


FIG. 6. As in Fig. 5 for the deuteron as the second excited state.

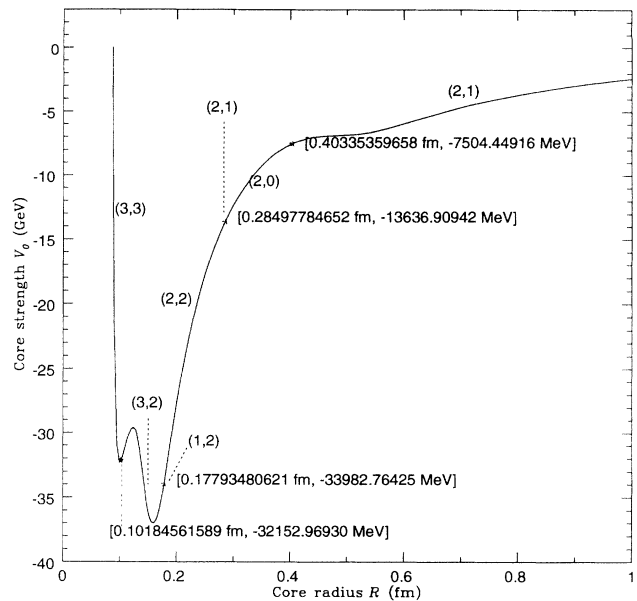


FIG. 7. As in Fig. 5 for the deuteron as the third excited state.

have a different number of nodes. When this is the case the nodes of u and w that remain will still occur at their previous locations. Exceptions occur in the transition regions where nodes are introduced or eliminated. For large values of R the central square-well character of the potential becomes dominant and the wave function approaches a pure S or D state.

IV. DISCUSSION

The model of the nucleon-nucleon interaction studied in this paper is an exaggerated one that imposes a clean separation between the exterior and interior parts of the potential. This is a simplification since there are various underlying processes leading to the potential function in coordinate space, and these processes generally result in knowledge of the interaction in overlapping regions. Nevertheless, it is of interest to determine how much of the deuteron can be understood with only the OPEP in the external region.

In contrast to the analyses of Friar *et al.* [3] and Ballot *et al.* [4], in which a pion-nucleon form factor is used to regularize the OPEP at the origin, our model retains more of the OPEP at shorter distances and allows for strong short-range interaction. The Friar central potentials become more repulsive inside 1 fm as the order m of the regularization increases from 1 to 10. The corresponding tensor force is weakened, with a minimum in the region of 0.1–0.5 fm. In the region beyond 0.5 fm the tensor forces are considerably weaker than pure OPEP but approach it as m increases. The deuteron binding energy is maintained by the interplay of stronger central repulsion and tensor attraction as m increases. In our approach the strong short-range tensor force is the dominant effect. We can obtain “reasonable” deuteron properties, although the effective range at the deuteron

TABLE III. Deuteron properties of the OPEP plus core potential of different depths. The deuteron is the second excited state of these potentials.

R (fm)	V_0 (MeV)	η	P_d (%)	r_D (fm)	Q_D (fm ²)	A_s (fm ^{-1/2})	ρ_α (fm)
0.1435074	-1000.00	0.02711	7.494	1.9483	0.2865	0.87432	1.703
0.1462245	-4000.00	0.02711	7.493	1.9481	0.2864	0.87426	1.703
0.1534158	-8000.00	0.02711	7.485	1.9476	0.2863	0.87402	1.701
0.1575460	-9000.00	0.02711	7.480	1.9472	0.2862	0.87384	1.700
0.1733165	-9987.23	0.02711	7.464	1.9454	0.2856	0.87305	1.696
0.2215493	-9000.00	0.02711	7.502	1.9446	0.2854	0.87265	1.693
0.3674381	-7000.00	0.02708	8.162	1.9429	0.2844	0.87194	1.689
0.4489938	-5000.00	0.02687	10.700	1.9067	0.2706	0.85575	1.589
0.7065090	-2000.00	0.02399	18.269	1.6891	0.1737	0.75761	0.835

pole and S -wave asymptotic amplitude are consistently on the low side. This is also characteristic of the results of Friar *et al.*

Although our model can produce wave functions with the same nodal structure as the Moscow potentials [5, 6], there is again an important difference. The potentials cited rely on a very strong central Gaussian attractive potential, $-1100 \exp[-(r/0.7)^2]$ MeV, for which there is no known physical origin, to produce the deep-lying Pauli-forbidden state. Since our understanding of the nuclear interaction is based on the one-boson exchange mechanism, it is difficult to believe that such a long-range scalar interaction which is many times deeper than OPEP even at 1.5 fm can exist. In the present model a similar wave function is produced through the tensor coupling mechanism which respects the hierarchy of force ranges, and without the need to invoke *ad hoc* components.

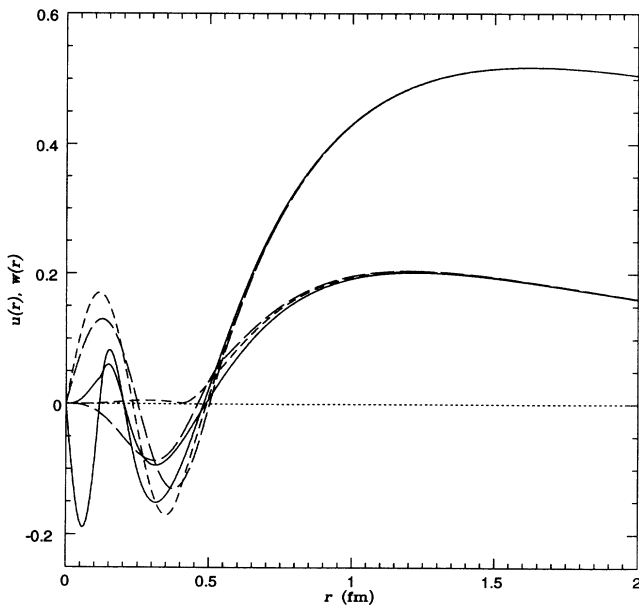


FIG. 8. Three wave functions representing the deuteron as the third excited state with different nodal structure. For the solid lines $R = 0.116$ fm and $V_0 = -30135.3235$ MeV, for the short-dashed lines $R = 0.4$ fm and $V_0 = -7571.86981$ MeV, and for the long-dashed lines $R = 0.55$ fm and $V_0 = -6534.31$ MeV.

There are other nucleon-nucleon interaction models that make a sharp separation between the interior and the exterior regions of the interaction. In the boundary condition model of Feshbach and Lomon [12], the interior part of the interaction is represented by the logarithmic derivative of the wave function at the core radius. The boundary conditions are independent of energy, but they do couple the S and D states. Although our model has energy-dependent logarithmic derivatives of the wave function at the core radius, tensor coupling occurs only in the exterior region through the OPEP.

As already mentioned, in our model the nodes of the wave function for potentials with sufficiently small core radii occur at the same place for the u and w functions and the locations of these nodes seem to be independent of the core strength (see Figs. 1–3). The deuteron static properties determine the external part of the wave function and are somewhat sensitive to the position of the outermost node(s), if there are any, but the deuteron properties do not allow one to distinguish between different behaviors of that part of the wave function inside the outermost node. Furthermore, the zeros of the two-nucleon wave function are quite insensitive to the energy of the scattering state. For example, we calculated the scattering states (up to 300 MeV) of the same potentials used to plot Fig. 1, and found that the nodes inside the potential region occur at exactly the same positions as for the “deuteron” wave function.

Beyond 1.5 fm, all the deuteron wave functions agree very closely, and even beyond 1 fm the differences are minor. This agrees with the conclusion of Klarsfeld *et al.* [10], who used methods independent of the short-distance nucleon-nucleon interaction to deduce a model-independent deuteron wave function consistent with its static observables. Other evidence for the essential determination of the deuteron wave function is provided by the comparison of wave functions determined by the many realistic potential models. Even models that incorporate explicit quark structure at small distances, such as Yamauchi and Wakamatsu [11], fall in this class; their final result agrees almost exactly with the Paris wave function. Where our present model falls short is in some lack of attraction in the intermediate-distance region near 1 fm, where empirical potentials incorporate some type of two-pion exchange interaction.

Looking at Tables I and III, we note that the trun-

cated OPEP tends to yield D -state probabilities which are larger than those of most realistic nucleon-nucleon potentials. Only when R is larger than 0.8 fm does the D -state probability approach the values of the realistic potentials. Realistic potentials which yield deuteron D -state probabilities that are on the large side tend to underbind the three-nucleon system [13], and thus one might conclude that the OPEP part of the potential is strictly valid only for distances greater than 0.8 fm. A careful phase shift analysis of the pp scattering data indicates that limiting the tail of the potential to the OPEP is reasonable only outside 1.8 fm [14].

There are recent suggestions that the charged-pion-nucleon coupling constant is smaller than given by earlier determinations [14, 15]. In Ref. [15] the fit to deuteron properties is used to obtain a 7% reduction of the coupling constant. The second to last line in Table I shows the effect of reducing the OPEP strength by 10% on the deuteron properties; this is to be compared with six lines above. Results of a recent phase shift analysis by Henneke [16], specifically the larger values of ϵ_1 for 50 and 100 MeV, however, suggest a stronger tensor force, i.e., less reduction of the OPEP tensor force by the ρ and other contributions.

V. CONCLUSION

The model of this paper explores the behavior of a quantum mechanical system with strong channel coupling. The various branches corresponding to different numbers of bound states yield wave functions which for large core radii approach either a pure S state or pure D state as R increases. The two possibilities alternate; i.e., for the single-bound-state branch it is the S , for the two-bound-state branch the D , etc. This reflects the fact that for large R the potential is predominantly a central square well in which the S and D bound states would alternate.

Another feature of note is the location of the nodes of the wave functions. When R is small the positions of the nodes of the S and D states are very nearly coincident and independent of the strength of the core (see Figs. 1, 2, and 3). The coincidence of the nodes of the u and w components of the wave function is the result of the strong coupling between the two functions, since at short distances the tensor component of the OPEP dominates and is much stronger than the centrifugal and the central parts. The behavior of the wave function when the tensor force dominates is discussed in the Appendix. The approximate analytic solution obtained there by neglecting all but the lowest-order term in the expansion of the potential bears remarkable similarity to the exact numerical solution. Indeed the presence of such a region in which the tensor force dominates seems to effectively screen the interior part of the potential. Different strengths and core sizes affect the deuteron properties little when the deuteron wave function has at least one node.

Only the outer part of the deuteron wave function is directly accessible to experiment. From Figs. 2 and 3 one sees that only the nodeless wave functions corresponding

to $R \gtrsim 1$ fm are qualitatively different; in all other cases the wave functions agree closely for $r \gtrsim 0.5$ fm. This is confirmed by the properties tabulated in Table I. The nodeless case leads to $P_d \sim 6\%$, and all the other cases to $P_d \sim 7.5\%$. These precise values are sensitive to the value of the coupling constant f^2 , and would be further tuned by introducing additional components to the outer potential. However, there is a clear qualitative difference between the two cases. It demonstrates that the usual deuteron properties are sensitive to the existence of a node in the wave function near 0.5 fm, but are insensitive to the details of the wave function inside that distance.

ACKNOWLEDGMENTS

We are grateful to NSERC Canada for continued support under research Grants Nos. OGP00-3198 (D.W.L.S. and E.W.) and OGP00-8672 (W.v.D. and E.W.). We are also indebted to DGICYT (Spain) for support under Grant No. PB91-0236 (J.M.), Contract No. 92/0021-C02-01 (P.S.), and for the award of a visiting professorship at the University of Barcelona in the spring terms of 1991 and 1992 (D.W.L.S.).

APPENDIX: BEHAVIOR OF THE WAVE FUNCTION AT SMALL DISTANCES

Here we present a simple model confirming our thesis that the behavior of the u and w components of the wave function at short distance is due to the dominance of the OPEP tensor force at short distances. Let us consider the Schrödinger equation for the two-nucleon system,

$$\left(\frac{d^2}{dr^2} - \alpha^2 - v_C \right) u = \sqrt{8}v_T w, \quad (\text{A1})$$

$$\left(\frac{d^2}{dr^2} - \alpha^2 - \frac{6}{r^2} - v_C + 2v_T \right) w = \sqrt{8}v_T u, \quad (\text{A2})$$

where v_C and v_T are the central and tensor parts of the OPEP when $r > R$, and α^2 is the deuteron binding energy in units of \hbar^2/m . Suppose that R is small and that we are considering values of r which also are small. In that case the terms involving v_T will dominate. For sufficiently small distances we can neglect the centrifugal term as well. The equations then become

$$\left(\frac{d^2}{dr^2} - \alpha^2 - v_C \right) u = \sqrt{8}v_T w, \quad (\text{A3})$$

$$\left(\frac{d^2}{dr^2} - \alpha^2 - v_C + 2v_T \right) w = \sqrt{8}v_T u. \quad (\text{A4})$$

These equations admit solutions for which the u and w functions are proportional to each other, i.e., $u(r) = aw(r)$ where a is a constant. The two possibilities are $a = \sqrt{2}$ or $-1/\sqrt{2}$. When $a = \sqrt{2}$, either $u(r)$ or $w(r)$ is the solution of the second-order differential equation

$$y'' - \alpha^2 y - (v_C + 2v_T)y = 0, \quad (\text{A5})$$

and when $a = -1/\sqrt{2}$, they are solutions of the equation

$$y'' - \alpha^2 y - (v_C - 4v_T)y = 0. \quad (\text{A6})$$

The general solutions of Eqs. (A5) and (A6) for $u(r)$ and $w(r)$ can be used to form a linear combination which is the general solution of Eqs. (A3) and (A4). Thus the system of coupled differential equations uncouples when the centrifugal term is dropped.

We do not have analytic solutions of Eqs. (A5) and (A6), but as we are considering small values of r we may further expand the potential about $r = 0$, giving

$$v_C + 2v_T = V_1 \left[\frac{6}{\mu^3 r^3} - 1 + \frac{3}{4} \mu r + \dots \right] \quad (\text{A7})$$

and

$$v_C - 4v_T = V_1 \left[-\frac{12}{\mu^3 r^3} + \frac{3}{\mu r} - 1 + \dots \right], \quad (\text{A8})$$

where

$$V_1 = -f^2 \mu c^2. \quad (\text{A9})$$

In both cases the $1/r^3$ term dominates the potential for small r ; in the first case the potential is strongly attractive, but in the second it is strongly repulsive. Keeping only the lowest-order term in r is equivalent to setting $v_C = 0$ and $v_T = -\kappa^2/r^3$, where κ^2 is a constant with dimensions length^{1/2}.

Neglecting further the α^2 term in Eqs. (A5) and (A6), we obtain the general solutions

$$u(r) = r^{1/2} \left\{ \sqrt{2} \left[C_1 J_1 \left(2\kappa \sqrt{\frac{2}{r}} \right) + C_2 Y_1 \left(2\kappa \sqrt{\frac{2}{r}} \right) \right] - \frac{1}{\sqrt{2}} \left[C_3 I_1 \left(\frac{4\kappa}{\sqrt{r}} \right) + C_4 K_1 \left(\frac{4\kappa}{\sqrt{r}} \right) \right] \right\}, \quad (\text{A10})$$

$$w(r) = r^{1/2} \left\{ C_1 J_1 \left(2\kappa \sqrt{\frac{2}{r}} \right) + C_2 Y_1 \left(2\kappa \sqrt{\frac{2}{r}} \right) + C_3 I_1 \left(\frac{4\kappa}{\sqrt{r}} \right) + C_4 K_1 \left(\frac{4\kappa}{\sqrt{r}} \right) \right\}, \quad (\text{A11})$$

where the C_i 's are constants of integration and the J, Y, K, I are cylindrical Bessel functions. In order to test the validity of the approximations, we consider the potential that gives rise to Fig. 3. Empirically, the wave functions exhibit oscillatory behavior rather than exponential growth and decay, and so we expect that C_3 and C_4 should be zero. Further, the I_1 and K_1 solutions arise from the repulsive potential Eq. (A6) and we expect these to be suppressed relative to the attractive potential of Eq. (A5). The value of κ is given by the potential strength and C_1 and C_2 are found by setting the wave function equal to zero at the core and by fitting one other nonzero point of the wave function in order to fix the normalization. The resulting analytic wave function is found to be very similar to the exact numerical solution up to the second outermost zero and only beyond that begins to deviate from the numerical wave function. Since the same constants C_i apply to both $u(r)$ and $w(r)$, they oscillate in phase.

In the case of soft-core potentials, e.g., that of Fig. 2, for which we observe that the wave functions are similar to those of the (small) hard-core potential, the behavior can also be understood in terms of the above solution. We see that again $C_3 = C_4 = 0$ because as r gets larger $\sqrt{r} I_1(4\kappa/\sqrt{r})$ approaches 2κ and $\sqrt{r} K_1(4\kappa/\sqrt{r})$ increases linearly with r . In this case the logarithmic derivatives of u and w inside the core must be matched with those outside the core at R . This matching condition determines R and one of the constants, say, C_2 . Then C_1 is fixed by the overall normalization. For small values of R and r the solution just outside R behaves as $r^{3/4}$ multiplied by a sine or cosine function. This agrees well with the observed progression of the heights of maxima.

The great strength of the tensor force at short distances, which is such that the centrifugal term of the potential can be neglected, explains the short-range behavior seen in the numerical solution of the hard-core and soft-core potentials. In particular the coincidence of the nodes of the u and w functions, the ratio of the u to w of very nearly $\sqrt{2}$, the clustering of the nodes near the origin, and the decrease of the amplitude as r approaches zero are all properties of the above analytic solution.

-
- [1] S. Klarsfeld, J. Martorell, and D.W.L. Sprung, Nucl. Phys. **A352**, 113 (1981).
[2] N.K. Glendenning and G. Kramer, Phys. Rev. **126**, 2159 (1962).
[3] J.L. Friar, B.F. Gibson, and G.L. Payne, Phys. Rev. C **30**, 1084 (1984).
[4] J.L. Ballot, A.M. Eiró, and M.R. Robilotta, Phys. Rev. C **40**, 1459 (1989).
[5] V.I. Kukulín and V.N. Pomerantsev, in *Contributed Papers from FEW BODY XII: 12th International Conference on Few Body Problems in Physics*, edited by B.K. Jennings (TRIUMF, Vancouver, 1989).
[6] V.I. Kukulín and V.N. Pomerantsev, Prog. Theor. Phys. **88**, 159 (1992).
[7] B. Buck, H. Friedrich, and C. Wheatley, Nucl. Phys. **A275**, 246 (1977).
[8] See, for example, R.D. Amado, F. Cannata, and J.P. Dedonder, Phys. Rev. C **41**, 1289 (1990).
[9] T.E.O. Ericson and M. Rosa-Clot, Phys. Lett. **110B**, 193 (1982); Nucl. Phys. **A405**, 497 (1983).
[10] S. Klarsfeld, J. Martorell, and D.W.L. Sprung, J. Phys. G **10**, 165 (1984).
[11] Y. Yamauchi and M. Wakamatsu, Nucl. Phys. **A457**, 621 (1986).
[12] H. Feshbach and E. Lomon, Phys. Rev. **102**, 891 (1956).
[13] R. Machleidt, Adv. Nucl. Phys. **19**, 189 (1989).
[14] J.R. Bergervoet, P.C. van Campen, T.A. Rijken, and J.J. de Swart, Phys. Rev. Lett. **59**, 2255 (1987).
[15] R. Machleidt and F. Sammarruca, Phys. Rev. Lett. **66**, 564 (1991).
[16] R. Henneck, Phys. Rev. C **47**, 1859 (1993).